Proceedings of the IASS 2022 Symposium affiliated with APCS 2022 conference
Innovation·Sustainability·Legacy
19 – 22 September 2022, Beijing, China

A Polyhedral Approach For The Design Of A Compression-Dominant, Double-Layered, Reciprocal Frame, Multi-Species Timber Shell

Zherui WANG*, Masoud AKBARZADEH[a]

*The University of Pennsylvania Weitzman School of Design
210 Meyerson Hall, South 34th Street, Philadelphia, PA 19104, USA
zheruiw@upenn.edu

[a]Polyhedral Structures Laboratory, Weitzman School of Design, the University of Pennsylvania

Abstract

With the advent of polyhedral 3D graphic statics, form-finding processes for multi-layered funicular shells can be attained with considerable ease by leveraging polyhedral reciprocal diagrams. Yet, the resulting space-frame structure consists of multiple structs converging at a single point, and demands a high degree of customization for the connecting node. This poses design, fabrication, and assembly challenges. Reciprocal frame (RF) [1] offers an alternative connection logic with added structural stiffness and aesthetic benefits. We present the design process of a timber frame prototype - a double layered, RF, compression-dominant, funicular shell. The paper, for the first time to our knowledge, applies the polyhedral form-finding method for a compression-only turned compression-dominant shell with RF. The prototype is designed with PolyFrame for Rhinoceros, fabricated by a 3-axis CNC machine and assembled with a 1-axis stacking logic. The optimal performative relationship between structural load, strut geometry, and principle axial stress of multiple wood species are investigated for the final prototype's material specification. The known complex RF geometric vs structural challenges found in free-form RF are addressed in relation to the funicular shell geometry given the varying strut lengths per node. The structural performance of the RF compressional-dominant shell prototype is numerically tested and compared with a conventional space-framed, compression-only shell of the same form. The workflow presented shows potential for application in multi-layered, structurally efficient, spatial structures with simplified fabrication and assembly process with locally sourced timber materials.

Keywords: Structural morphology, reciprocal frame, 3-dimensional graphic statics, compression dominant structure, furnicalar shell

1. Introduction

With the advent of polyhedral 3-dimensional graphic statics (3DGS), form-finding processes for multi-layered funicular shells can be attained with considerable ease by leveraging polyhedral reciprocal diagrams. However, the resulting space-frame structure consists of multiple structs converging at a single point, and demands a high degree of customization for the connecting node. This poses design challenges, and requires high degrees of customizations for fabrication – all of which further complicates the assembly process – especially for multi-layered shell structures with at least four struts approaching the node at multiple planes and angles. While additive manufacturing advancement in the past decade has offered customizable, 3d-printed joints [2], printing can be costly and is not necessarily available or accessible for all designers. Through adaptive casting techniques, molds can respond to local nodes and strut angles [3]; however, the embodied carbon expenditure with casting materials like concrete exert considerable environmental impact. With the resurgence of timber as structural design materials, some studies resolve multi-nodal conditions by harnessing natural variation of found tree-folk [4], but valence may be limited by available stock for a multi-layered spatial structure.

Working with standard dimensional timber elements, we are proposing to resolve the node design by leveraging the benefit of two-bar-only connection afforded by reciprocal frames (RF) for a double-layered, compression-dominant, multi-species timber shell structure informed by finite subdivision of force polygon. Working with limited machinery access, the proposed RF elements can be fabricated with 3-axis CNC mills or conventional band saws. By combining RF and the 3DGS form-finding process, the proposed shell prototype benefits from the added stiffness and compression-dominant load path, while expanding RF to the multi-layer configurations and aesthetic expressions.

1.2. Related works

This section reviews the relevant literature on polyhedral 3DGS and RF as two distinct research topics. Known geometric and structural considerations are highlighted in relation to the design integration of the method proposed in this paper.

1.2.1. Polyhedral 3-dimensional graphic statics

Recent developments in polyhedral 3DGS have expanded designers' capacities to design spatial structures visually and intuitively through the form and force dualities in three-dimensional space. For the polyhedral approach [5], force equilibrium is achieved by closing the corresponding force polyhedron. By mapping force vertices to form polyhedra, force edges to form faces, force faces to form edges, and force polyhedra to form vertices through Minkowski transformation, all form edges converge at the normal direction of force faces, and experience compression or tension-only forces with no or little bending.

Supported by polyhedral 3DGS, previous works have used flat sheet panels [6], and kerf bending and zipper joints [7] to materialize multi-layered spatial structures and resolve complex nodal articulation problems. As exemplified in the Kerf bending method – a bending technique where curvature is achieved through intermittent kerfs – a total of 6 members are needed for a 4 strut node, where each strut consists of three interlocking members with highly customized zipper tooth patterns (Figure 1.a). This is to say that although multi-strut nodes can be rationalized and fabricated with standard machinery, the design and assembly process still poses challenges. This paper complements previous works on double-layered, funicular shells by exploring their compression-dominant RF relative with the added benefit of aesthetics, simplified fabrication and assembly, and nodal stiffness. Although the customized nodal connectors are no longer required to accommodate all struts, RF introduces eccentricity and additional geometric and structural uncertainties on its own.

1.2.2. Reciprocal frame structures

With the origin from both Leonardo da Vinci's sketch, *Codex Atlanticus*, and ancient Chinese bridge construction as depicted in water color painting, *Along the River During the Qingming Festival*, the structural morphology of RF as part of a free-form surface has been studied widely in the past decades [1]. Larsen *et al.* documented the design and construction of a full scale timber exhibition hall with beams polar arrayed around an oculus [8]. Thönnissen *et al.* leveraged RF as part of intertwining single layer lattice structures. Apolinarska *et al.* devised a funnel-shaped canopy where the structural integrity of the overall freeform is achieved by balancing normal force and displacement at the joints, and RF node opening [9]. Gherardini *et al.* reviewed a wide range of undulating and doubly curved surfaces modulated by RF [10]. Most of the studies have benefited from similar bar lengths that affords a greater degree of flexibility in reducing eccentricity of connecting members. Studies on double-layered RF are comparatively limited, particularly for non-flat, curved systems. Noting the added benefit of flexural stiffness, Kohlhammer *et al.* analyzed the structural load of double-layer free-form RF structure, where upper and lower chords are connected by a Delauney truss logic [11]. The studies concluded that the ultimate load of upper and lower layers is inversely proportional to the node opening [11].

While RF structures have been studied extensively, most literature focuses on a free-form, single-layer surface topology, through which the uncertain structural behavior of the overall form is predominantly justified by flexural stiffness at the nodal scale. Assisted by the subdivision of the global force polyhedral diagram, we are proposing to 3-dimensionalize RF structure into a double-layered, compression-dominant shell, where the design of the overall form is visually guided by the 3DGS funicular form-finding workflow. With this approach, the structural behavior at the scales of global form and of the node are synergistically considered throughout the design process. Yet, with edges derived from the 3DGS form-finding process rotated to free multiple struts converging at a single point, the compression-only force flow is disrupted. The structural performance of a compression-dominant, funicular, RF shell in comparison with its compressional-only, spaceframe counterpart is addressed in Section 3.

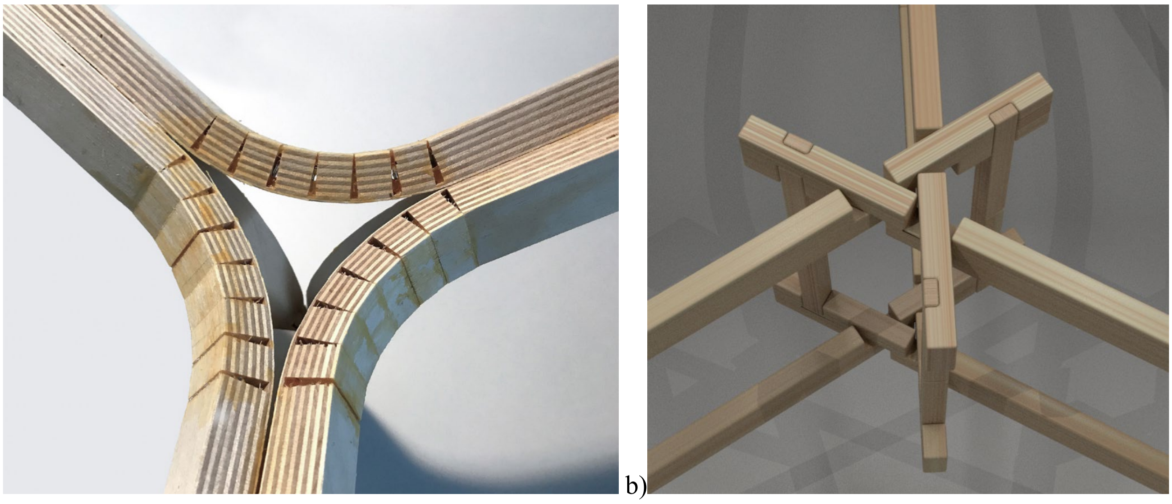

Figure 1: a) Example of a Kerf bending node designed with polyhedral 3DGS [7]. b) Proposed reciprocal frame node designed with polyhedral 3DGS.

2. Methodology

This section introduces the computational design and fabrication process for a double-layer funicular shell with RF at converging nodes. The proposed design flow begins with a compression-only shell composed of linear strut elements generated with the polyhedral-based 3DGS technique. The struts are rotated at the midpoint to reduce multi-struct nodes to two-strut RF. While the technique can be applied to a board category of multi-layer synclastic shells, the prototype structure shown in Figure 2 is used as a reference to the design process below. To demonstrate the feasibility of the design process, the algorithm is applied to a double-layered shell morphology as exemplified in Figure 10.

The overall design and fabrication process is as following, and the resulting shell is shown in Figure 2:

1. We use PolyFrame, a Rhinoceros-based plugin [12], to design the double-layer, funicular shell via form-force reciprocal diagrams based on our previous work on polygon subdivision [13].
2. The resulting edges are rotated counter-clockwise on the x-y-plane at each node to reduce the diversity of intersecting plane orientations.

3. Edges are materialized with linear wood elements. For the upper and lower layer of the shell, the sizing of the struts is balanced by their principal axial stress, allowable stress of the wood species, and geometric constraint of eccentricity.
4. The vertical edge connecting two shell layers is translated in the direction of corresponding upper and lower members. This process is repeated per the number of converging struts per shell layer. Its sizing is one-third of the force load for each interlayer member.
5. Notch joints connect two neighboring struts either on the same or bridging between two shell layers. RF allows mutual support of connecting structs during the assembly process.
6. Struts are fabricated with 3-axis CNC without flip-mill procedures to reduce fabrication time and complexity.
7. Assembly of the struts with a z-axis only stacking logic to avoid complex spatial maneuvers of the members during the erection process.

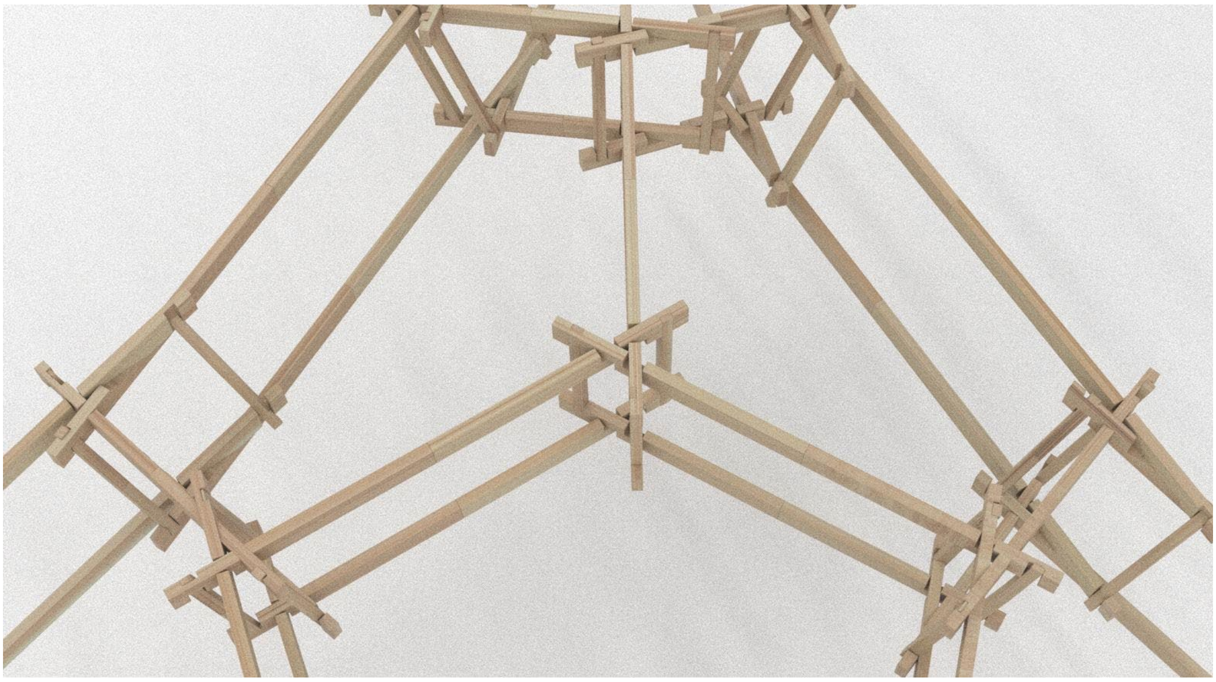

Figure 2: Aerial view of a doubled layered, reciprocal frame, compression dominant shell.

2.1. Double-layer funicular shell geometry generation

To acquire the double-layer funicular shell, we devised a triangular pyramid as the force diagram where the applied loads and reactions correspond to the base and three sides of the polygon respectively (Figure 3.a). This results in a synclastic configuration with three supports. To generate multi-layered shell structure, each face corresponding to the forces were subdivided with the barycentric subdivision logic into smaller force polygons. While the location of the applied forces changes, the overall magnitude of the reaction and applied forces remains the same. The internal cells of the force polyhedron are subdivided with the same ruleset, in which case the overall force is preserved, while the direction and magnitude of the internal shell changes. This suggests that the internal force polyhedral cells may produce a topologically different form compared to its overall exterior face, such that for the form diagram, the angles between edges may differ significantly at nodes close to the shell boundary (Figure 3b). This poses challenges for devising RF connections while reconciling the eccentricity between two structs spatially, because the struts at the shell boundary are significantly longer than that of the interior, and their adjacent angles are usually substantially shallower. To mitigate potential geometric complications, where the eccentricity of connecting struts is simultaneously constrained by the shell curvature, struts length, and strut x-y plane orientation derived from the force diagram, we divided the global form diagram into the interior and exterior chunks at the shell boundary, where two separate operations are applied to generate RFs (Figure 3.b). In this manner, two RF lattices intertwine to form a single RF shell. The two exploded RF lattices and their combined configuration in forming a single shell is shown in Figure 3.c.

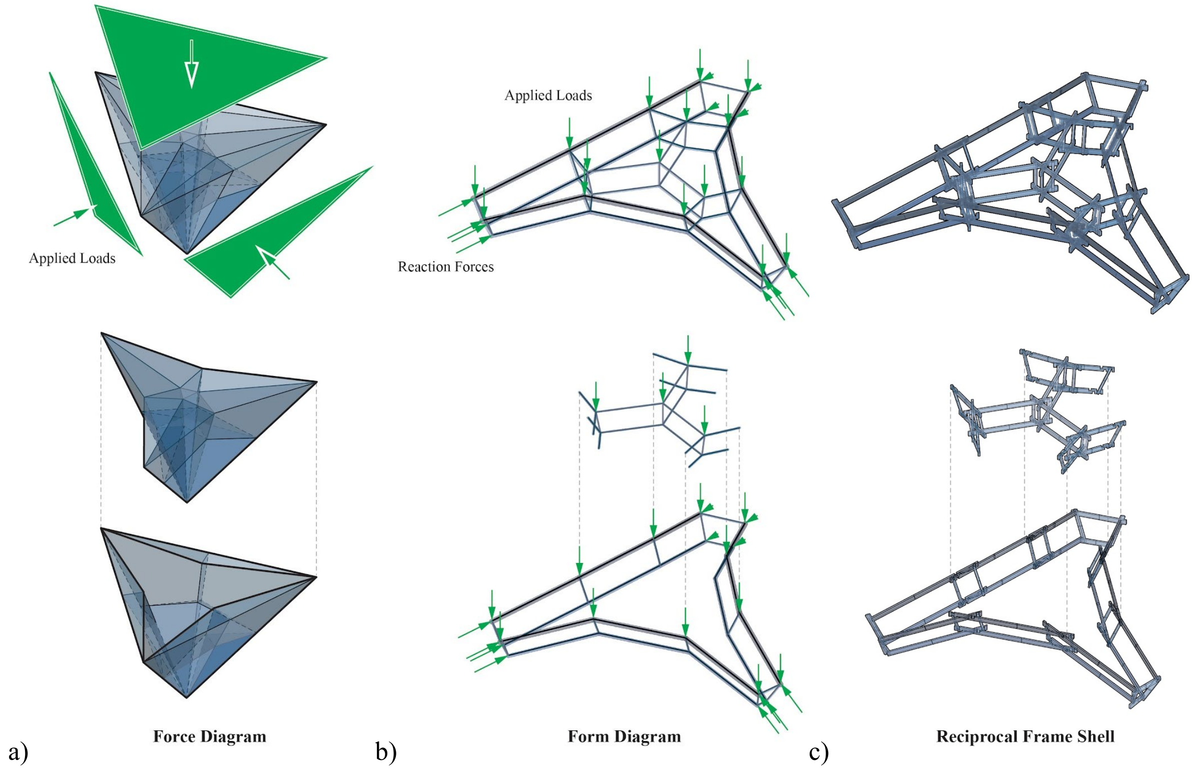

Figure 3: Intertwined compression-dominant, RF, double-layered shell derived from the form-force reciprocal diagram of the compression-only, double-layered shell. a) Force diagram and separated at the shell boundary. b) Corresponding form diagram and exploding at the shell boundary. c) Two reciprocal frame lattices intertwine to form a single shell.

2.2. Reciprocal frame nodal scale articulation

To devise the RF node from the form diagram, we used nodes and edges illustrated in Figure 4.a for a single layer shell. Figure 4.b to 4.h shows step-by-step procedure. For starters, all available edges derived from PolyFrame are sorted to identify shared connecting nodes. Each edge is then rotated counterclockwise at its center point. To minimize the eccentricity due to different edge lengths at a single node, a cylinder is generated at the node for each of the edges, such that the edge is rotated up to the tangent point of the cylinder (Figure 4.c). This ensures that RF node opening is not disproportionately skewed towards any edge directions, and each pair of connecting structs would have enough intersecting volumes and contact areas for interlocking joints. Using the volumetric intersection between each pair of connecting struts as a template, the bite area of the notch joint is simplified to a rectangular profile parallel to the x-y plane in order to eliminate undercuts for CNC milling (Figure 4.f). This ensures the notches can be fabricated without the flip-milling procedure. Subsequently, these rectangular profiles are extruded in the z-axis – a direction conforming to the edge rotation axis – to allow the notched bite surfaces to be parallel to strut surfaces at all times (Figure 4.g). In this manner, all structs can be assembled by stacking in a single axis.

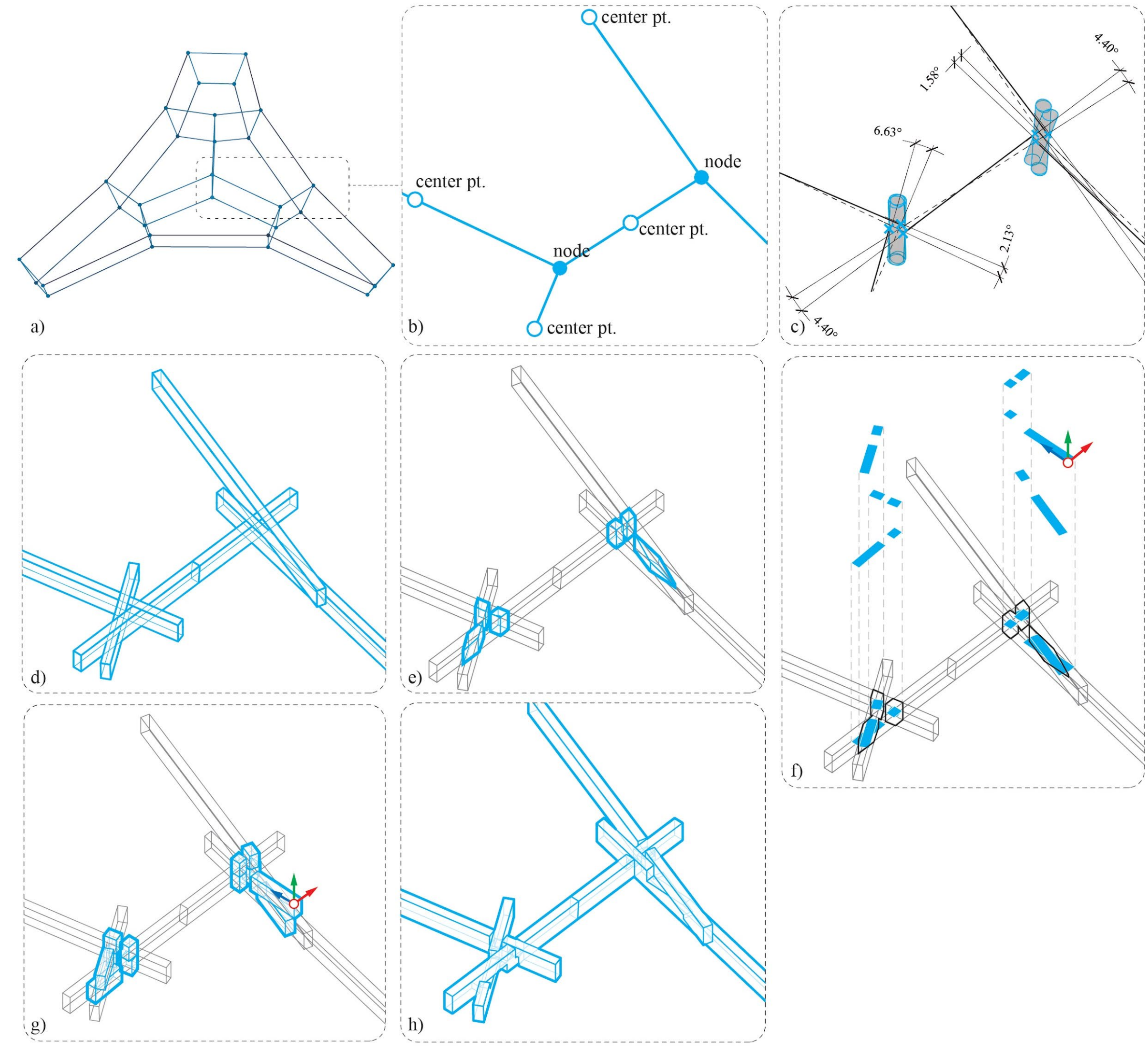

Figure 4: Design process of the upper layer of the shell with input edges obtained from the form diagram. a) Double layered, compression-only shell obtained from the form diagram, b) edges, their center points and shared connecting nodes, c) rotational angle deduced from the edge and tangent of the cylinder, d) rectangular structs generated based on the new edge, e) material intersection of the connecting structs, f) simplified bite surface outline projected to the xy plane, g) notch joint negative volumes extruded based on the bite surface, h) resulting RF node with notch joints.

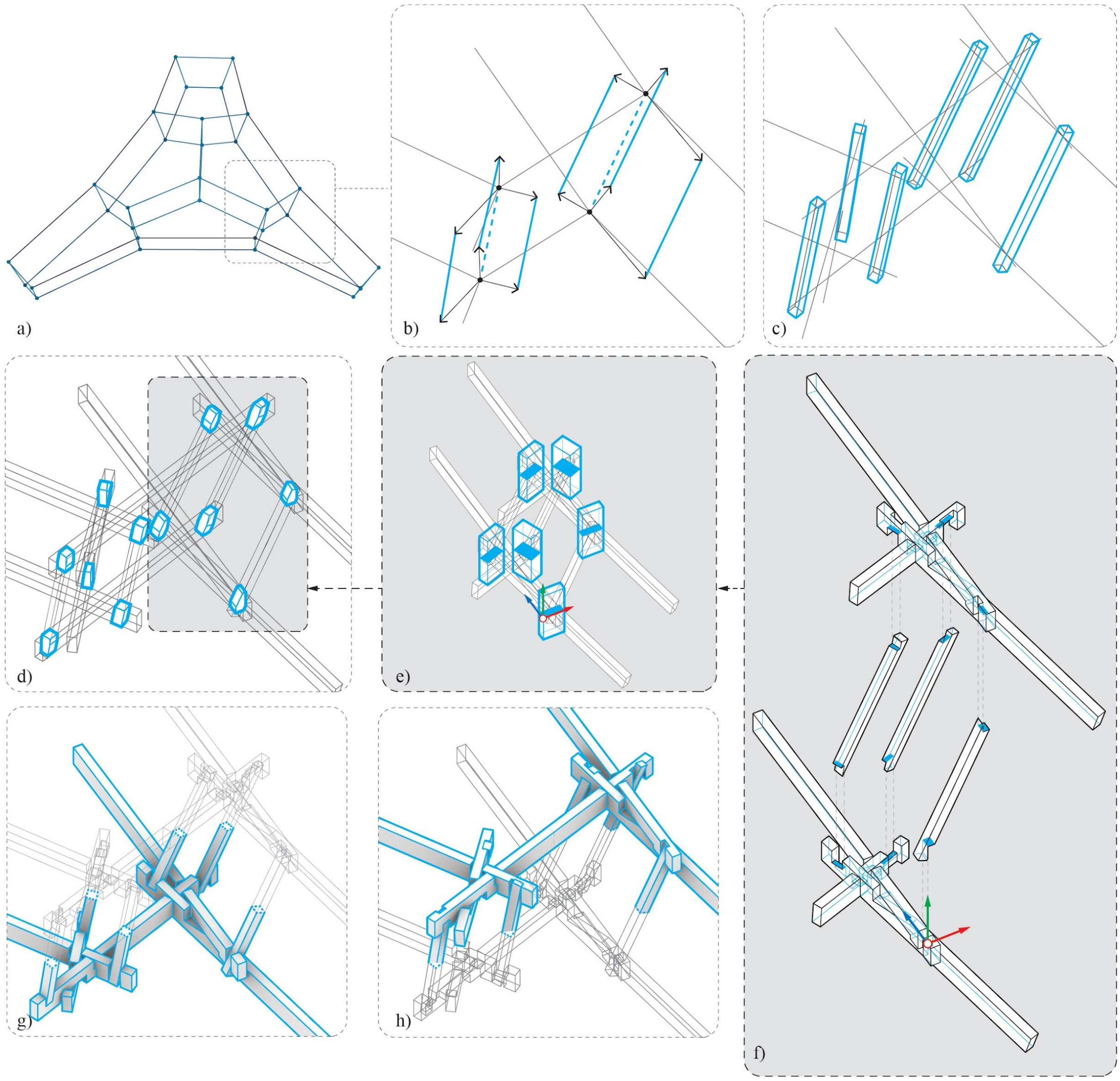

Figure 5: Step-by-step procedure to resolve the connecting structs between the upper and lower shell layers. a) Double layered, compression-only shell obtained from the form diagram, b) inter-shell-layer edge translated three times, c) structs generation, d) intersection volumes of the connecting structs, e) simplified bite surface parallel to the xy-plane, f) 1-axis stacking assembly of the upper and lower shell layers connected by notched joints, g) resulting RF node at the lower shell layer, h) resulting RF node at the upper layer shell layer.

To bridge the upper and lower shell layers, the connecting edge is translated to each of the shell edge directions (Figure 5.b). The force magnitude embedded in the curve is reduced to ⅓ of the original. The connection logic for the inter-shell-layer struts remains the same as the shell layers – each notched and interlocked to their neighbors with bite surfaces parallel to the xy-plane.

2.3. Strut sizing and wood species co-optimization

Given the compression-dominant nature of the force flow, the struts are sized according to the principal axial stress based on the magnitude of forces obtained from the form-finding process. The width of the members is maintained while the depth increases proportional to applied loads and magnitude of force flow network.

While RF structures typically consist of similarly sized members, presumably due to the redundancy of members and graded force magnitudes across the free-from surface, the form and force distribution of our proposed compression-dominant, RF, funicular shell depends on the subdivision logic of the force diagram, where the force magnitude between neighboring struts may differ greatly, especially at the shell boundary. Figure 6.a illustrates the substantial strut depth difference, particularly for a node at the shell boundary, if all struts are materialized by a single wood species with a uniform compression strength. To reduce struts size difference at a node, the strut depth is optimized against the compression strength of wood species (Table 1). With varying material densities, the strut depth demand is compensated by the material strength, such that the sizing of perimeter struts at shell boundaries can be reduced to its material limit. In order to minimize the embodied transport carbon of the timber during the construction process, four wood species – bass, aspen, northern red oak, and white birch – are down-selected based on their availability in locally-harvested forests in the Commonwealth of Pennsylvania. As shown in Figure 6.b, with white birch, the shell perimeter struts become shallower than their neighbors. The final strut sizing strategy (Figure 6.c) seeks to balance uniformity of struts depth to ensure similar material contact area for joint bite, while simultaneously selecting the wood species that can sustain the required compressive loads. Figure 7 illustrates the change of strut species across the double-layer shell structure for six different applied load scenarios. While the struct sizing and the overall shell configurations are maintained, the strut wood species shifts as applied load increases.

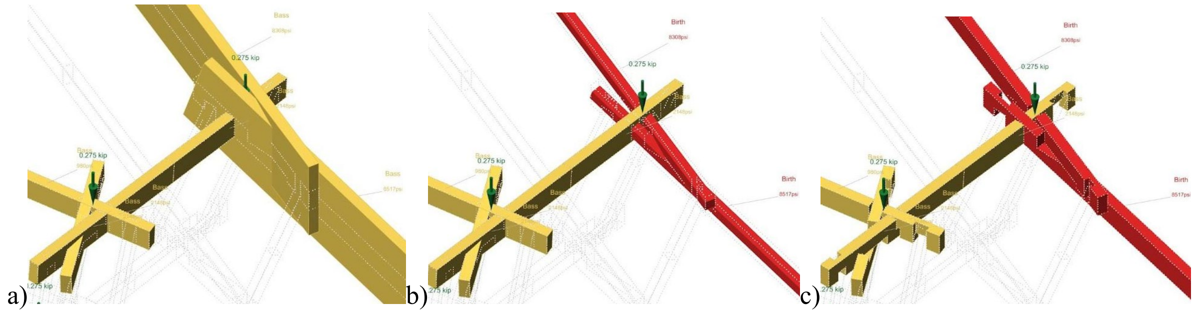

Figure 6: Strut cross section depth of the upper layer of the shell is sized per a) principle axial stress with bass, b) wood species with the least material volume, and c) overall depth uniformity across all members.

Wood Species	Compression Parallel to Grain (kPa)
Bass	32600
Aspen	36500
Sycamore	37000
Yellow Poplar	38200
Cucumber Magnolia	43500
Northern Red Oak	48500
Sugar Maple	54000
Yellow Birch	56300
White Birch	59000

Table 1: A list of wood species and corresponding compression strength parallel to the grain direction [14]. The highlighted species in blue are locally sourced options in the Commonwealth of Pennsylvania.

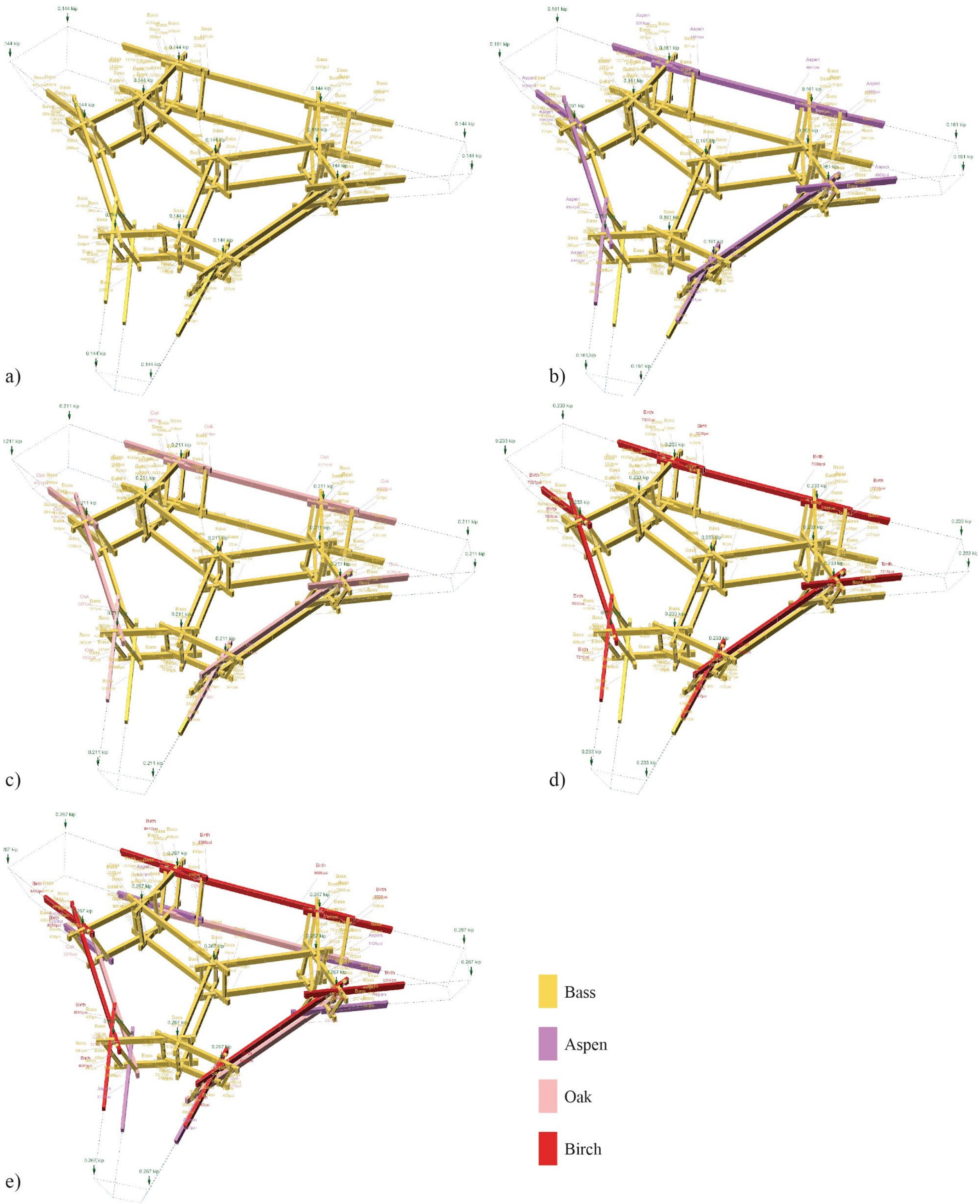

Figure 7: Compression-dominant, double-layered, RF, funicular shell under incremental applied loads from a) to e) through which struts are materialized with wood species of increasing compressive strength.

3. Structural analysis comparison

Finite element analysis is conducted to compare a typical double-layer node articulated with space frames and with RF. A total load of 1kN is applied to the node of the top shell layer, while the upper and lower layer struts are fixed at the end. Compared to the spaceframe node, the RF node experiences less Von Mises stress by a magnitude of 10 fold (Figure 8), and 12.5% less maximal displacement (Figure 9).

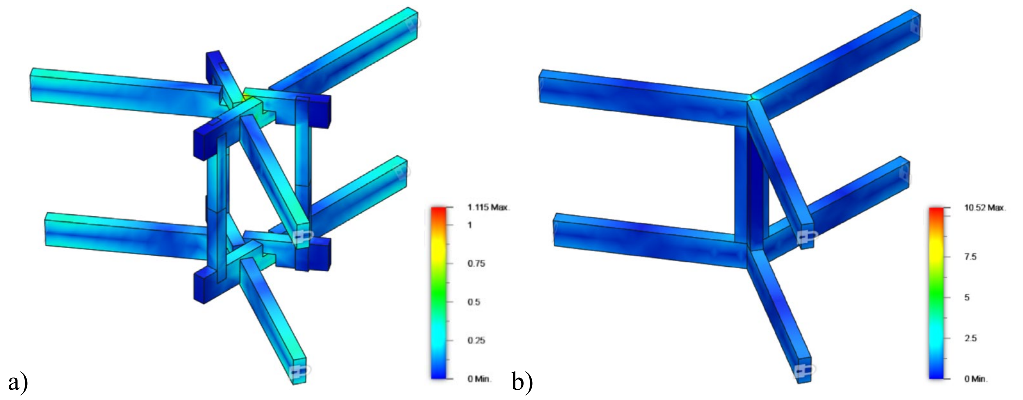

Figure 8: Von Mises stress exhibited in a single, double-layer node for a) , and b) conventional space frame.

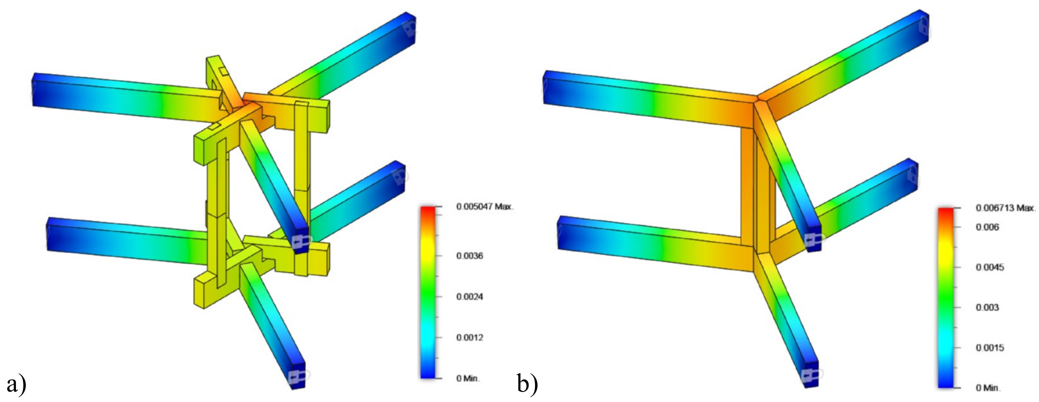

Figure 9: Displacement exhibited in a single, double-layer node for a) RF, and b) conventional space frame.

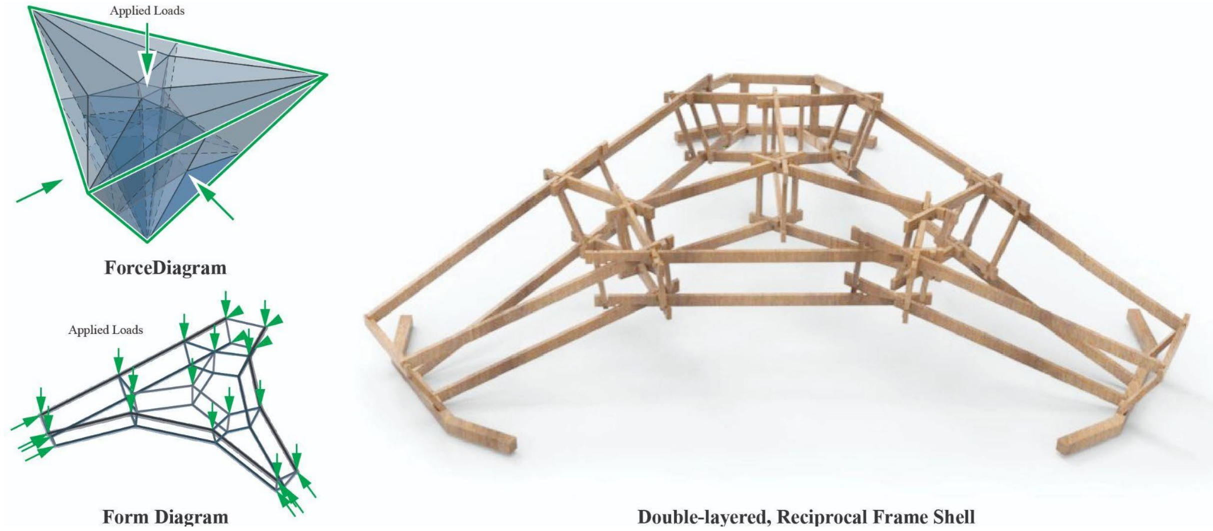

Figure 10: The complete shell accompanied by the form-force reciprocal diagram.

4. Conclusion and outlook

This paper presents a new design method that applies polyhedral-based 3DGS form-finding to a compression-only turned compression-dominant, double-layered shell with RF. With RF, the number of custom nodes and structural elements connecting multiple edges are significantly reduced. The challenge of eccentricity known to RF and the wide range of force magnitudes found in shells generated with polyhedral subdivision are mitigated with globally calibrated struct size and varying compression strength of wood species. In order to streamline the assembly process, notched joints are devised to facilitate 1-axis stacking logic that both simplifies the spatial maneuver of structs during the shell erection process and reduces the reliance on mechanical fasteners commonly found in butt joint connections – a practice further opens up the potential for the ease of disassembly or material recycling for future studies. In comparison with the double-layered spaceframe, the structural performance benefit of a double-layered RF is confirmed with numerical analysis at the node scale. A comprehensive structural analysis for the entire shell is anticipated for future studies. With structurally considered assembly sequence, the proposed design method opens up the potential of constructing multi-layered, funicular spatial shell structures with reduced formworks – a topic that warrants future research.

References

[1] A. Pugnale and M. Sassone, "Structural Reciprocity: Critical Overview and Promising Research/Design Issues," *Nexus Netw. J.*, vol. 16, no. 1, pp. 9–35, Apr. 2014.

[2] P. Bedarf, I. Kontiza, and T. Spathi, "Spatial Graded Patterns: A case study for large-scale differentiated space frame structures utilising high-speed 3D-printed joints," in *Proceedings of the 36th eCAADe Conference*, Lodz, Poland, Sep. 2018, vol. 2, pp. 39–46.

[3] A. Baghi, "FLEXI-NODE," in *Proceedings of the 39th Annual Conference of the Association for Computer Aided Design in Architecture*, Austin, Texas, 2019, pp. 207–218.

[4] P. Von Buelow, O. Oliyan Torghabehi, S. Mankouche, and K. Vliet, "Combining parametric form generation and design exploration to produce a wooden reticulated shell using natural tree crotches," in *Proceedings of the IASS Symposium 2018*, Boston, Jul. 2018, vol. 1.

[5] M. Akbarzadeh, T. V. Mele, and P. Block, "Three-dimensional Compression Form Finding through Subdivision," p. 7, 2015.

[6] Y. Lu *et al.*, "All glass, compression-dominant polyhedral bridge prototype: form-finding and fabrication," in *Proceedings of the IASS Annual Symposium 2020/21 and the 7 th International*

Conference on Spatial Structures, Guilford, UK, Aug. 2021, p. 11.
[7] Y. Liu, Y. Lu, and M. Akbarzadeh, “Kerf Bending and Zipper in Spatial Timber Tectonics: A Polyhedral Timber Space Frame System Manufacturable by 3-Axis CNC Milling Machine,” presented at the Realignments: Toward Critical Computation, Online and Global, Nov. 2021.
[8] O. P. Larsen, *Reciprocal Frame Architecture*, 1st ed. London: Routledge, 2007.
[9] A. A. Apolinarska, M. Kuhn, F. Gramazio, and M. Kohler, “Performance-Driven Design of a Reciprocal Frame Canopy,” in *Proceedings of the 39th eCAADe Conference*, Novi Sad, Serbia, 2021, vol. 1, pp. 497–504.
[10] F. Gherardini and F. Leali, “Reciprocal Frames in Temporary Structures: An Aesthetical and Parametric Investigation,” *Nexus Netw. J.*, vol. 19, no. 3, pp. 741–762, Dec. 2017.
[11] T. Kohlhammer, A. A. Apolinarska, F. Gramazio, and M. Kohler, “Design and structural analysis of complex timber structures with glued T-joint connections for robotic assembly,” *Int. J. Space Struct.*, vol. 32, no. 3–4, pp. 199–215, Jun. 2017, doi: 10.1177/0266351117746268.
[12] A. Nejur and M. Akbarzadeh, “PolyFrame, Efficient Computation for 3D Graphic Statics,” *Comput.-Aided Des.*, vol. 134, May 2021.
[13] M. Akbarzadeh, T. Van Mele, and P. Block, “Compression-only Form finding through Finite Subdivision of the Force Polygon,” presented at the Shells, Membranes and Spatial Structures: Footprints”, Brasilia, Brazil, Sep. 2014.
[14] D. W. Green, J. E. Winandy, and D. E. Kretschmann, “Mechanical Properties of Wood,” in *Wood Handbook: Wood as an Engineering Material*, Centennial., Madison, Wisconsin: United States Department of Agriculture Forest Service, 2010, pp. 5–1 to 5–3.